Effect of Volcanic Ash on Durability and Performance of Thermal Barrier Coatings in Gas Turbine Engines

[a] Prakash C. Patnaik, [b] Kuiying Chen and [c] Mike Graham

[a] Gas Turbine Laboratory, Aerospace Portfolio, National Research Council Canada
[b] Structures, Materials and Manufacturing Laboratory, Aerospace Portfolio, National Research Council Canada
[c] Researcher Emeritus, National Research Council Canada
(CANADA)

Prakash.patnaik@nrc-cnrc.gc.ca and Kuiying.chen@nrc-cnrc.gc.ca

ABSTRACT

Thermal barrier coatings (TBCs) are highly complicated material systems applied on hot engine components to reduce the impact of prolonged heat attack by using thermal insulating materials. Aircraft engines can encounter the attack from volcanic ash resulting in molten deposits to TBC spallation and premature degradation of hot section components. The molten glass deposits degrade the top coat of TBCs, and thus ultimately reduce the lifetime of gas turbine engines.

This paper studies theoretically and numerically the degradation of TBCs under attack by volcanic ash. During the attack process, volcanic ash penetrates the columnar structure of the EB-PVD (Electron Beam Physical Vapor Deposition) TBC top coat in a similar way as CMAS (Calcium Aluminum Magnesium Silicate). As the compositions of volcanic ash differ with respect to geographical location, it is difficult to design TBCs that can effectively resist such ash attack. At lower operating temperatures, the ash adheres to top coat surface and leads to premature degradation. After penetrating to a certain depth, volcanic ash facilitates delamination of the top coat, and due to an accumulation of stress, the columnar structures near the sintering edges crack.

One output of paper is the prediction of delamination maps of the TBC top coat due to volcanic ash penetration. It allows us to better understand the delamination mechanism that could lead to failure. Moreover, it can also provide potential guidance in designing effective TBCs that could better resist the damage caused by volcanic ash infiltration.

1.0 INTRODUCTION

It has long been recognized that gas turbine engine components normally suffer from severe impact of corrosion and oxidation caused by hot combustion gases. For an engine to perform at higher efficiency, it should operate at the highest allowable temperature [1-3]. An application of TBCs on turbine blades can partially inhibit these effects by reducing the surface temperature of metallic engine components by ~100-300^{o}C.

Volcanic ash ingested in the engine intake air collides with the surface of TBCs, adheres to the coating surface and melts at high temperatures. These ash particulates fill vertical gaps in the top coat and react with TBC constituents. Volcanic ash reacts with the top coat in a similar way as the CMAS (Calcium Magnesium Alumina Silicates) does and degrades the performance of TBCs. The two vulnerable deposits that cause failure of TBCs are sulphate and CMAS glassy deposits. At low temperatures, these substances cause physical

damage through high-velocity impact. At high temperatures, they react with TBC constituents and form undesirable chemical compounds.

2.0 CALCIUM MAGNESIUM ALUMINA SILICATE (CMAS) AND ITS IMPACT ON TBCS

CMAS is a readily available airborne dust particle that acts as a kind of environmental deposit. It is a hard micro glass, and often used to test TBC durability. The CMAS enters the TBC system through the pores and gaps distributed at the top coat surface. At high temperatures, the CMAS reacts with the TBC and causes ZrO_2 grains to dissolve [4,5]. Therefore, reducing surface porosity and gaps could become an approach to mitigate the CMAS degradation on TBCs.

If the temperature of the top coat exceeds the melting point (1240 ^{o}C) of CMAS [6-9], the CMAS melts and penetrates into the top coat due to its excellent wetting properties. When the TBC temperature drops during cooling, it causes a residual stress in the top coat due to a difference of coefficient of thermal expansion between the CMAS and the top coat. Upon the temperature dropping below the CMAS melting point, the molten CMAS forms a denser layer in the top coat. Figure 2-1 shows the delamination cracks parallel to the top coat surface in a TBC [6]. These cracks are distributed within the areas filled by CMAS. During cooling, solidification of CMAS in the penetrated region results in high in-plane stiffness in the dense layer [6]. The tensile stress generated during this process is released in the form of delamination cracks, Figure 2-1a.

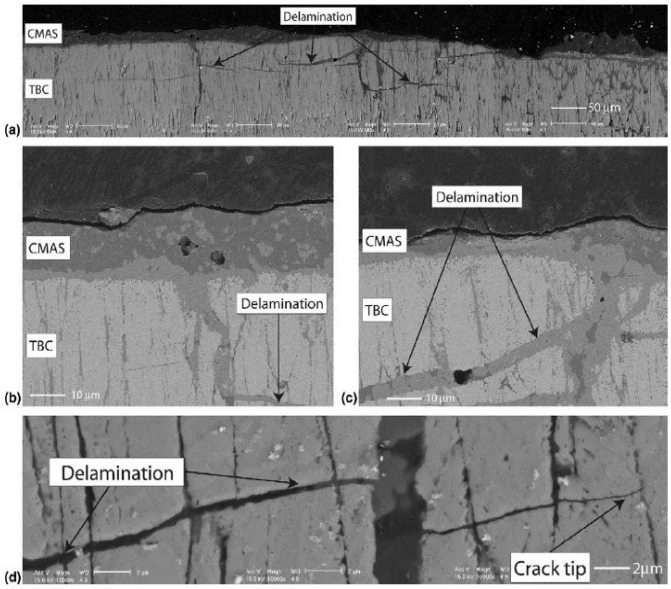

Figure 2-1: (a) Black scattered electron image of region with delamination cracks. (b) Electron image with phase contrast at interface TBC/CMAS. (c) Electron image with phase contrast in CMAS infiltrated crack. (d) CMAS infiltrated crack. Inter columnar gaps on both sides of the crack remain aligned meaning the delamination is strictly mode I [6].

It is concluded [7,10] that the vertical cracks in the top coat can initiate a delamination, and this delamination is dictated by the mode I crack, in which the crack propagation direction is normal to the tensile stress. The delamination of TBC due to CMAS attack depends on several factors [8] such as : 1) temperature and thermally induced stress; 2) channel cracking and penetration of these cracks into the CMAS region. Thermally induced stresses can be caused by temperature gradients which could arise from a sudden cooling of coating surface during engine shutdown period [11].

3.0 VOLCANIC ASH AND ITS EFFECTS ON TBCS

Volcanic ash is a mixture of pulverized rock, mineral and glass that spreads out in atmosphere during volcanic eruption, and is generally formed during an eruption of a volcano. The dissolved gases in magma expand and escape violently into the atmosphere, and then solidify into fragments of volcanic rock and glass [12], and eventually expand into the clouds and can prevail in the atmosphere for months.

The attack on TBC by volcanic ash is a serious threat to the aviation industry. Typically volcanic ash is hard and abrasive in nature. Sulphur compounds and other aerosols can be found in ash particles. At high altitudes, due to the temperature being below zero, the ash particles freeze. When an aircraft passes through a cloud of volcanic ash, it causes wear to propeller blades and turbo-compressors of the aircraft. The volcanic ash has the capability to cause an engine flameout because it contaminates the fuel and water system of the plane. However, the primary reason of engine flameout associated with volcanic ash attack is the deposition of ash on hot section components in the engine [13]. Due to this deposition, there is a rapid increase in both static burner pressure and compressor discharge pressure. As a result, there is a restriction of air movement in the engine. Abrasive particles can erode blades of the compressor, which leads to a decrease in the pressure of the air fed to the engine combustor, thus reducing the efficiency of the engine and inducing a loss of thrust.

The composition of volcanic ash mainly depends on the type of minerals present in the magma. Materials and minerals in the ash are based on the type of volcanic magma and the geographic location of a volcano. In the case of a volcanic eruption, pyroclastic materials are formed due to accelerated fragmentation of dissolved volatile components. Volcanic ashes are formed from these pyroclastic materials. The density of these ash particles can vary from 700 to 3200 Kg/m^3, especially the molten glass particles formed from volcanic ash, have a density of around 2350–2450 Kg/m^3.

It was known that delamination and penetration are two major ways by which the volcanic ash is prone to affect TBC durability. The delamination of the top coat by volcanic ash attack occurs only when the ash penetrates the top coat to a certain depth [14]. As a comparison, Figure 3-1 shows the Scanning Electron Microscopy (SEM) microstructure of the TBC fabricated by EB-PVD without ash attack, while Figure 3-2 shows the volcanic ash attack on TBC during thermal cycles at 1250℃, resulting in deposition of volcanic ash ($30mg/cm^2$) over the top coat.

It is difficult to differentiate a volcanic ash cloud from a normal cloud when in flight. If the aircraft is in contact with volcanic ash, it could lose power to the engines [16].

Figure 3-3 shows the damaged high pressure rotor blades of an aeroplane after it encountered volcanic ash. Even though the degradation mechanism of volcanic ash on TBC is similar to CMAS, researchers have struggled to predict the nature of damage. This paper deals with the effect of volcanic ash on the durability and performance of TBCs of gas turbine engines. The main focus is to identify the conditions which lead to

crack propagation in TBCs due to volcanic ash infiltration. The temperature range needed for delamination to occur by volcanic ash, and essential thermal gradients needed to protect the TBC are identified in this study. It is expected that the established delamination maps can be used to develop more durable TBCs.

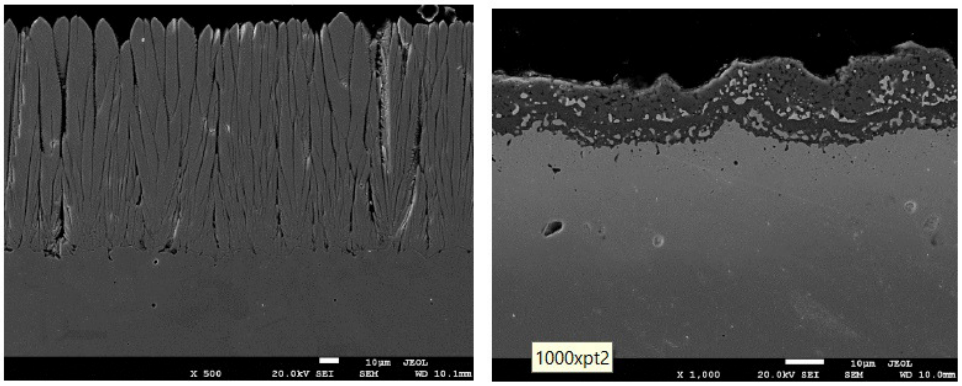

Figure 3-1: SEM image of unaffected TBCs[15]. Figure 3-2: SEM image of TBC after 30 minutes of ash attack at 1250℃ [15].

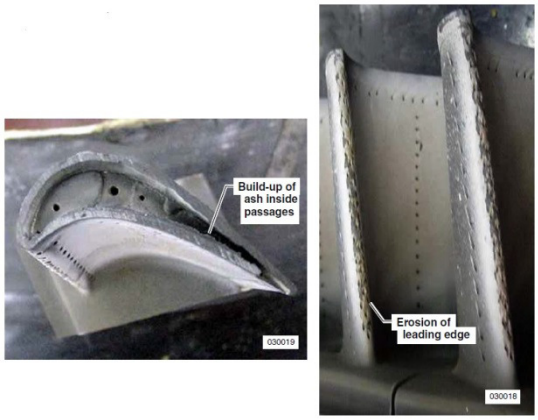

Figure 3-3: High pressure rotor blade of NASA DC8 airplane engine after ash encounter [16].

4.0 THEORY AND METHODOLOGY

To study the delamination of TBCs by volcanic ash attack, the fracture mechanics combining thermal gradient effect was applied [11]. A geometry model used to study the delamination of TBC is constructed consisting of three layers as shown in Figure 4-1. A dense layer penetrated by ash into the top coat is refereed to the layer I with a thickness h. The top coat without ash penetration is refereed to the layer II with a thickness H-h, while the layer III represents the substrate. Delamination of TBC occurs, for example, at a height d within the top coat, parallel to the TBC surface. The initial surface temperature of the top coat is assumed as $T^{i}_{surface}$, while the initial interface temperature to the substrate as $T^{i}_{substrate.}$ For the top coat, the Young's modulus, Poisson's ratio, thermal conductivity and diffusivity coefficient are denoted as E_2, ν_2, k_2, κ_2 respectively. These quantities for the dense layer are represented by E_1, ν_1, k_1, κ_1 respectively.

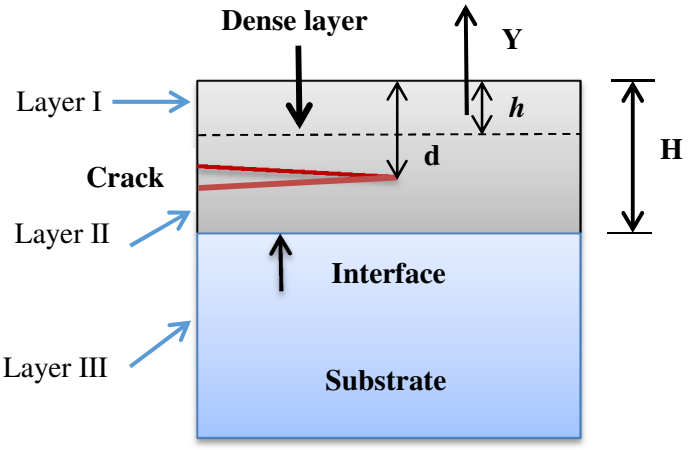

Figure 4-1: Schematic geometry model of three-layer coating system used to study its delamination.

Evans and Hutchinson [11] predicted that the delamination of the top coat under the CMAS attack would be predominant in two regions, 1) shallow delamination within the dense layer; 2) deep delamination under the dense layer above the substrate. Their model is primarily based on the following assumptions: 1) TBC experiences sufficient creep and the stress relaxation occurs at operating temperatures; 2) engine shuts down rapidly while the TBC material responds thermo-elastically; 3) vertical separations are present from the surface to the substrate.

To study the crack propagation, the mode I delamination is considered, with the mode I toughness $\Gamma_{IC}^{(1)}$ for the dense layer and the toughness $\Gamma_{IC}^{(2)}$ for the unaffected top coat (Jm^{-2}). The dependence of toughness Γ_C^i on mode mixture is given by [11],

$$\Gamma_C^i = \Gamma_{IC}^i[1+\tan^2((1-\lambda)\psi)] \ . \qquad (1)$$

where Γ_{IC}^i is the mode I toughness at the interface. The phase angle ψ is determined by stress intensity factors K_I and K_{II} through $\psi = \tan^{-1}(K_{II}/K_I)$. The delamination mode also depends on the mixed mode parameter λ ($0<\lambda<1$).

The temperature distribution at equilibrium within the TBC is described as,

$$T(\eta) = A(\eta)T_{surface} + B(\eta)T_{substrate} \qquad (2)$$

where $\eta = y/H$ describing the fraction coordinate, and y is the coordinate shown in Figure 4-1. $A(\eta)$ and $B(\eta)$ are two geometry related parameters, with $A(\eta) = 1+C_1\eta$, $B(\eta) = 1-C_2\eta$, $C_1 = \dfrac{k_2/k_1}{1-h/H(1-k_2/k_1)}$, and $C_2 = \dfrac{1}{1-h/H(1-k_2/k_1)}$.

The biaxial in-plane stress associated with the cooling parameter Φ is given by [11],

$$\sigma(\eta) = \frac{E_1 \alpha_{coating} \Delta T_{sur/sub}}{1-\upsilon_1}\{1 + C_1\eta - \Phi\} \quad \text{in the dense layer,} \tag{3}$$

$$= \frac{E_2 \alpha_{coating} \Delta T_{sur/sub}}{1-\upsilon_2}\{C_2(1+\eta) - \Phi\} \quad \text{in the coating below the dense layer} \tag{4}$$

With $\Phi = \Delta\alpha\Delta T_{sub} / \alpha_{coating}\Delta T_{sur/sub}$. Two stress intensity factors are calculated by [11],

$$K_I = \frac{P}{\sqrt{2Ah}}\cos\omega + \frac{M}{\sqrt{2Ih^3}}\sin\omega$$
$$K_{II} = \frac{P}{\sqrt{2Ah}}\sin\omega - \frac{M}{\sqrt{2Ih^3}}\cos\omega \tag{5}$$

where $A=\lambda+\Sigma$, $\Sigma = ((1+\alpha_D)/(1-\alpha_D))$. α_D is the Dundurs' elastic mismatch parameter. Symbol I represents the moment of inertia of the bilayer (layer I + layer II). The force/length $P = \int_{-d}^{0} \sigma(y)dy$ and the moment/length $M = \int_{-d}^{0} \sigma(y)(D+y)dy$.

At the transient state, the temperature distribution $T(y, t)$ in the TBC is calculated by [11],

$$T(y,t) = T^i_{surface} - (T^i_{surface} - T^f_{surface})erfc\left(-y/2\sqrt{kt}\right) \tag{6}$$

where $erfc(x)$ is the complimentary error function. The associated biaxial stress can be evaluated as,

$$\sigma(y,t) = \frac{E\alpha(T^i_{surface} - T^f_{surface})}{1-\upsilon} erfc(-y/2\sqrt{kt}) \tag{7}$$

The thermal stress $\sigma(T,t)$ can be calculated in terms of Young's modulus E_1, thermal expansion coefficient $\alpha_{substrate}$ and Poisson's ratio ν_1 [11],

$$\sigma(T,t) = \frac{E_1[\alpha_{coating}(T^i(\eta) - T(\eta,t)) - \alpha_{substrate}(T^i_{substare} - T_{substrate}(t))]}{1-\nu_1} \tag{8}$$

The deep delamination in homogenous coating can be calculate at $d/H = 1$. The associated steady state energy release rate G for crack propagation is given by [11],

$$G = \frac{H}{6\overline{E_2}}(3\overline{\sigma}^2 + \sigma_0^2), \tag{9}$$

where $\overline{\sigma} = E_2\alpha_{caoting}\Delta T_{sur/sub}(0.5-\Phi)/(1-\nu_2)$ and $\sigma_o = [E_2\alpha_{coating}\Delta T_{sur/sub}/2(1-\nu_2)]$. The bar in the

expression denotes the plane strain modulus $\overline{E} = E/(1-\nu^2)$.

For shallow delamination, at which $d/H < 1$, it is assumed that the delamination strictly undergoes the mode I type, it follows $P > 0$ and $M > 0$. The associated energy release rate G is then evaluated by [11],

$$\frac{G}{[(1+\nu_2)/(1-\nu_2)]E_2 H(\alpha_{coating}\Delta T_{sur/sub})^2} = 0.176(1-\Phi)^3 \quad . \qquad (10)$$

For mode I crack to propagate in a homogeneous coating, the cooling parameter satisfies : $0 < \Phi < 0.275$ [11]. During the initial cooling, $\Phi = 0$, the mode I delamination cracks do not exist within the TBC. The delamination develops only after the substrate has cooled sufficiently, *i.e.* $\phi \geq 0.275$. When this happens, the energy release rate G reaches the maximum, and the delamination takes place along the interface. With further cooling of the coating, the energy release rate decreases, and the delamination crack propagates towards the surface of the top coat.

5.0 THEORY RESULTS AND DISCUSSIONS

The maximum operating temperature of TBCs used in gas turbine engines is restricted by several factors such as the sintering of the top coat, thermal cyclic durability of the TBC and deposits of volcanic ash [8]. At high temperatures, the ash melts and wets the TBC surface and then, due to capillary action, gets sucked into the open void spaces that exist within the TBC. High thermal gradient across the TBC can lead to the formation of residual stress that in turn leads to TBC delamination. The residual stress formed during TBC operation depends on the difference in cooling efficiency between the top coat surface and the substrate [6].

Tensile residual stress is generated in TBC system during engine shutdown. It is known that TBC layers are made from different materials with different thermo-mechanical properties, as a result, the CTE mismatch between these layers may occur. The CTE mismatch and thermal gradient play an important role in determining the delamination cracks and their propagations of TBC infiltrated with volcanic ash.

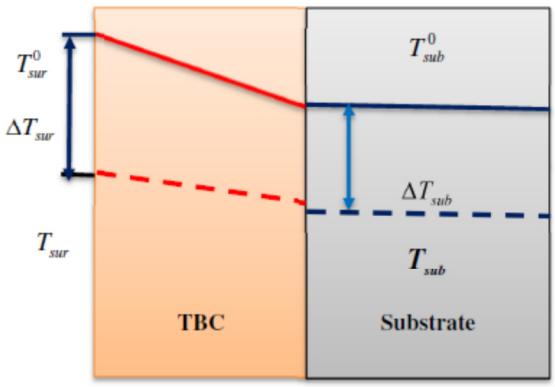

Figure 5-1: Temperature parameters used in the calculations.

In Figure 5-1, T^o_{sur} is the initial surface temperature of a TBC during engine operation. The initial temperature

of substrate is set to T^{o}_{sub}. The temperature difference between these two initials is represented by $\Delta T_{o} = T^{o}_{surf} - T^{o}_{sub}$. The temperature drop $\Delta T_{sur/\ sub} = \Delta T_{sur} - \Delta T_{sub}$ is defined as the difference between the temperatures changes of ΔT_{sur} in the top coat and ΔT_{sub} in the substrate. This temperature drop defines the response of the top coat surface and the substrate to thermal gradient occurring during engine operation.

Figure 5-2 illustrates the delamination map of TBC calculated using the formula (10). Delamination map can be used to evaluate a possible engine operation path, in which the fail-free and safety path could be obtained. In Figure 5-2, the areas of shaded region outside each curve, for specific λ value (such as λ=0.3, 0.5, 1.0) represent the TBC delamination areas, while the non-shaded area or the area inside the curve represents a delamination-free region or a safe region for the respective curve. The delamination map in Figure 5-2 is plotted against a mixed mode crack parameter λ. Dotted lines in Figure 5-2 represent selected cooling trajectories.

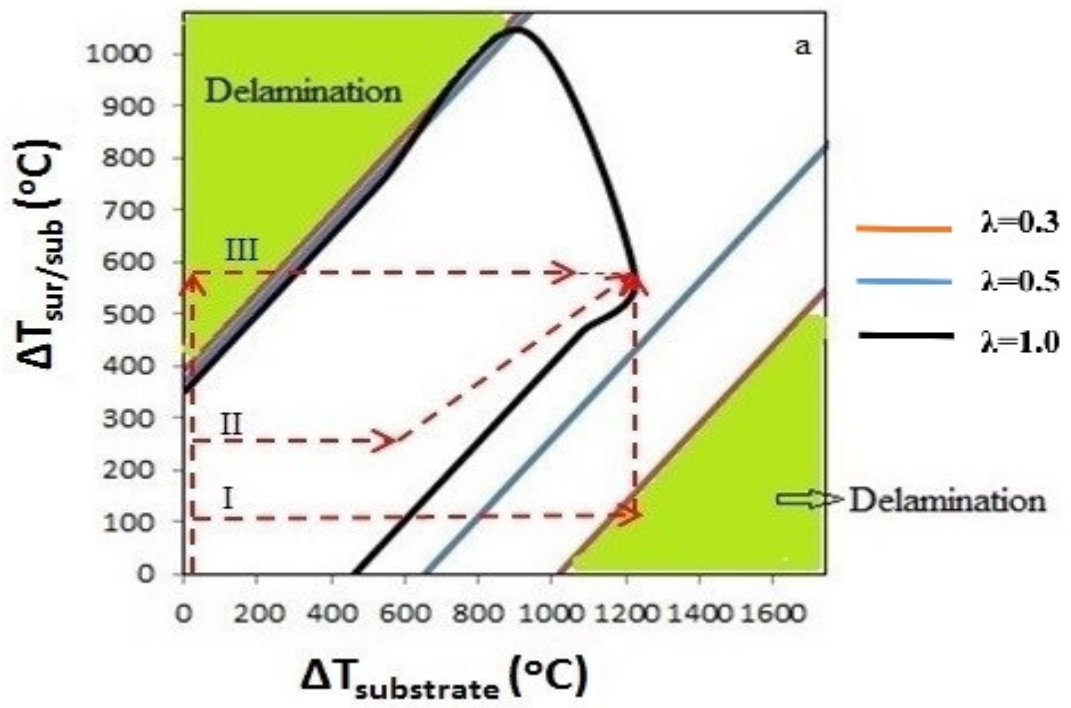

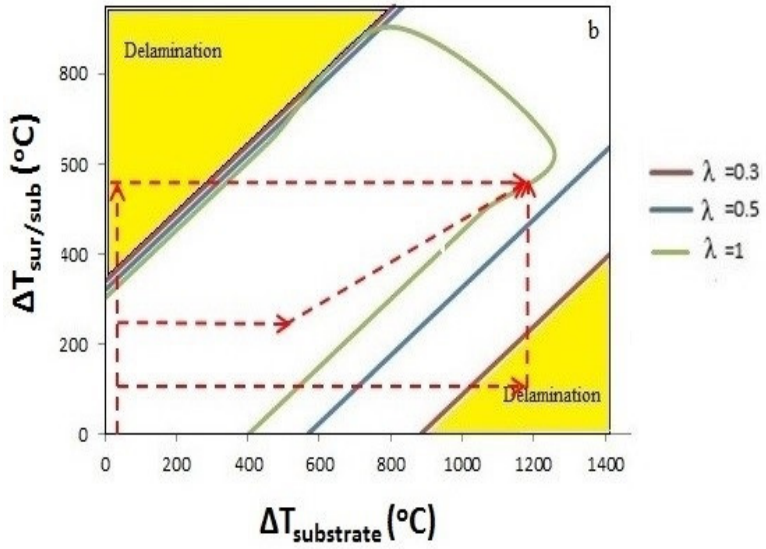

Figure 5-2: Delamination maps for homogenous coating system at equilibrium consisting of three trajectories I, II and III: a) λ= 0.3, λ= 0.5, λ= 1 with mode I toughness = 60 J/m^2, b) λ= 0.3, λ= 0.5, λ= 1 with mode I toughness = 40.

The cooling of the TBC system can be conducted in many ways, for instance, in three ways as indicated for I, II and III in the figure. The trajectory I in Figure 5-2 defines a cooling path that initially keeps the top coat surface temperature unchanged while reduces the substrate temperature. After this path reaching the delamination area as indicated in the figure, the trajectory I switches and remains this substrate temperature but reduces the top coat surface temperature to a point in the non-delamination region. The trajectory III in Figure 5-2 defines another cooling path that initially reduces the top coat surface high temperature while keeps the substrate temperature unchanged. After this path III reaching another delamination region, it also switches and keeps this surface temperature unchanged but reduces the substrate high temperature to a point in the non-delamination region. The trajectory path II is a mixture of the trajectory path I and the trajectory path III, but this mixture path III processes entirely in the non-delamination region.

Considering the plot for λ=1 of pure mode I failure, the TBC system operates following the cooling trajectories I and III, from the initial starting point, to the destination as indicated by arrows in Figure 5-2. These two cooling trajectories I and III were identified to enter the delamination areas, consequently, the system fails. In trajectory I, the surface temperature initially remained constant, while the substrate temperature decreases significantly, represented by $\Delta T_{substrate}$. This cooling path preliminarily simulates an internal cooling scenario of blades, followed by the engine shutdown. In trajectory III, the substrate temperature is kept at constant, followed by a significant surface temperature drop $\Delta T_{sur/sub}$. The trajectory II cooling path is a fail-safe process, as the cooling curve entirely falls within the boundaries of the non-delamination region.

To our knowledge, there are no results available on delamination maps related to volcanic ash attack, evaluated in terms of thermal gradient formulae. Our delamination map regarding volcanic ash attack on TBC system is evaluated based on the formulation (10). The present TBC systems consist of both the homogenous top coat without dense layer infiltrated with ash and a bilayer of top coat with one dense layer infiltrated by ash and one normal top coat, Figure 5-2. Two more conditions were investigated: one, the delamination toughness was varied while volcanic ash penetration depth was kept at constant; and in the second case,

volcanic ash penetration depth varies. In Figure 5-2, the specific layer thickness for the top coat H = 165 μm and the dense layer h= 50 μm were selected in the TBC delamination evaluations.

Table 5-1: Thermal mechanical properties for TBCs used to evaluate delamination.

	Young's modulus (GPa)	Thermal Expansion coefficient (ppm/℃)	Poisson ratio	Mode I delamination toughness (J/m^2)
As-Deposited TBC	40	11	0.2	30-60
Volcanic ash penetrated substrate	400	85	0.2	30-60
CMAS Penetrated substrate	200	11	0.2	30-45

Table 5-1 lists thermal and mechanical properties for both volcanic ash and CMAS [16,17,11]. Figures 5-2 (a) and (b) show the delamination maps obtained for volcanic ash attack on TBC. Here λ represents the mixed crack mode parameter as discussed in the proceeding sections. The map is obtained for delamination under homogenous coating system for three crack mode parameter values, λ=0.3, 0.5 and 1.0 and for two different mode I toughness values of 40 J/m^2 and 60 J/m^2, respectively. It was observed that, for the same toughness parameter λ, increasing fracture toughness of the coating from 40 J/m^2 to 60 J/m^2 in (a) and (b), will increase the area of safety region illustrated by the shaded areas.

To study the delamination occurring during cooling process, we investigated two cooling scenarios for volcanic ash attack on TBCs, i) engine power is reduced, cooling air at substrate temperature is suddenly introduced on surface coating and then allowing both coating and substrate to cool down uniformly; ii) uniform cooling down of the entire system and eliminating temperature gradient. The curve λ=1 is taken for consideration as an example.

Similar discussions can be made for other λ values, which represent other crack mode scenarios. As shown in Figure 5-2, the cooling trajectories I and III fall under the first cooling scenario.

Regions outside the black curve in Figure 5-2 (a) represent the delamination region for λ=1, while the area inside the curve is the safe region. The cooling curves I and III enter the delamination region, respectively, while the cooling curve II is safe as it falls entirely under the safe region where there is no delamination. For λ<1, as an indicator of mode mixture of I and II cracking scenario, the delamination areas represented by shaded regions are shrunk, demonstrating that as long as the shear crack mode II is involved, the delamination tendency of the coatings is restrained to some extent.

Using this method of analyzing cooling trajectories in delamination map, we can find the possible best cooling trajectory for the TBC system that does not cause its delamination. The data obtained can be used in designing a TBC system and in defining the engine operation with a safety path for efficient working performance. As discussed, Figure 5-2 (b) shows a similar delamination map for different fracture toughness values.

In addition to the development of the delamination map of TBCs at the steady-state, we further studied the transient temperature distribution and its effect on the TBC delamination. In the present study, these maps were plotted for two different cases. First, we varied toughness while keeping volcanic ash penetration depth constant. In this case as shown in Figure 5-3, three different mode I toughness values were used: 30 J/m^2, 45J/m^2, 60J/m^2 against the in-plane modulus of top coat E = 40 GPa.

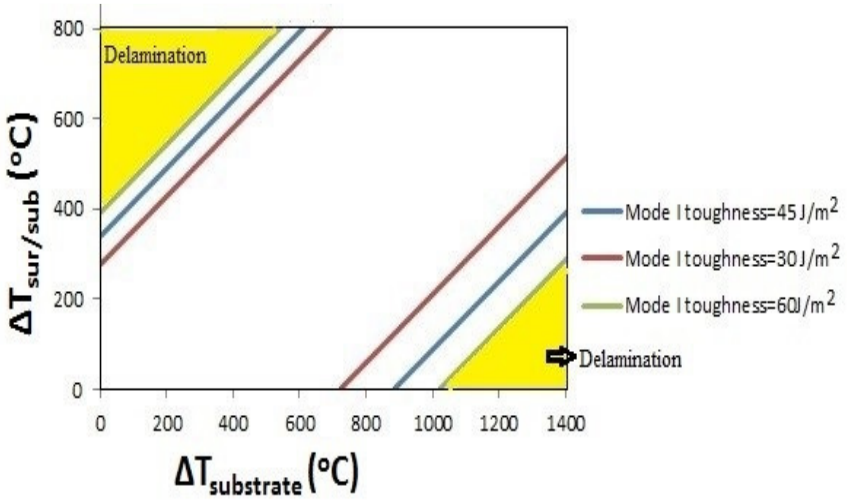

Figure 5-3: Delamination map for different mode I toughness.

According to Figure 5-3, as the mode I toughness is increased from 30 J/m^2 to 45 J/m^2 and to 60 J/m^2, the difference in $\Delta T_{sur/sub}$ also increases subsequently, indicating that the safety region also increases. This trend in the transient temperature distribution is the same as in the steady-state situations. It defines a wide temperature region, in which the engine can operate without occurrence of TBC delamination. In technical terms, it means that the temperature drop between the top coat surface and the substrate can be larger for TBCs with higher toughness without causing delamination.

By using different toughness, we can also determine the approximate temperatures of the substrate, from which we can predict whether the system would be damaged or not under these operating conditions. We vary the depth of volcanic ash penetration in TBC with three different values of h/H= 0.3, h/H= 0.5 and h/H= 1.

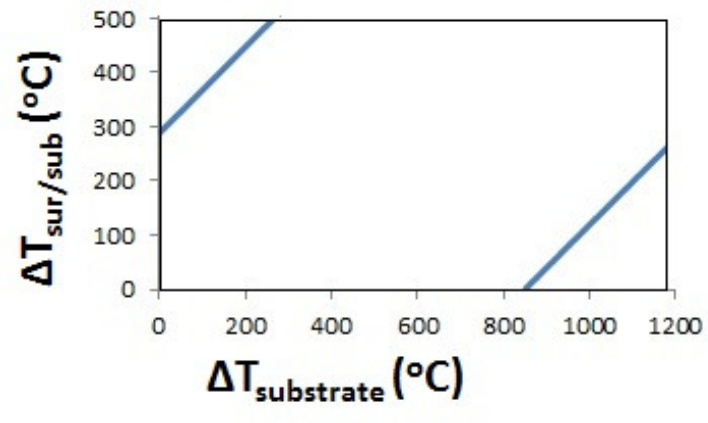

Figure 5-4: Delamination map for *h*/*H*=0.5.

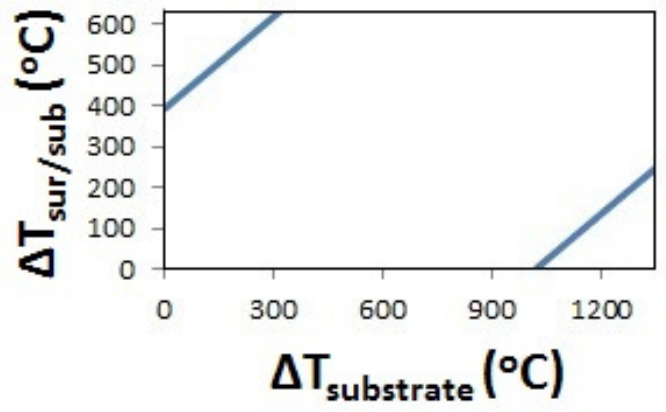

Figure 5-5: Delamination map for *h*/*H*=0.3.

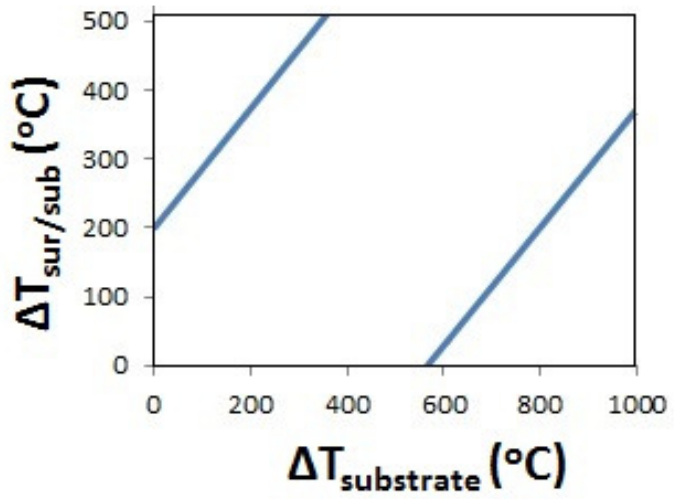

Figure 5-6: Delamination map for *h*/*H*=1.

Figures 5-4, 5-5 and 5-6 were used to find the allowable temperature windows ($\Delta T_{sur/sub}$) for the TBCs with or without a dense layer. The allowable temperature windows allow us to predict the likely temperature drop and the substrate temperature that do not cause TBC delamination during engine operation. The substrate temperature can then be used to identify whether the system falls in the delamination region or not. If there is no allowable temperature window, i.e. $\Delta T_{sur/sub}$ = 0, then the substrate temperature is equal to the surface temperature, leading to the delamination. In Figures 5-4, 5-5 and 5-6, when the allowable temperatures of 300℃, 400℃ and 200℃ are applied, the substrate temperatures are 850℃, 950℃ and 600℃ approximately, which correspond to the delamination safe region. The results drawn from Figures 5-4, 5-5 and 5-6 can be used to find the safe operating temperature windows for TBCs. Higher operating temperatures result in higher efficiency of the engine operation.

The effect of volcanic ash on TBC durability is similar to that of the artificial CMAS, but it is more intense and severe because of its complicated structure and varying composition. More importantly, the larger elastic modulus will in turn facilitate the delamination crack formation and TBC failure. Since the penetration could happen at a faster rate, volcanic ash quickly infiltrates the columnar structure of the EB-PVD ceramic top coat. From the delamination map obtained above, the delamination caused by volcanic ash infiltration could occur much earlier than the CMAS. Both the CMAS and volcanic ash delamination models may predict the safe operating temperatures close to each other. The model for ash delamination predicts that, the system would be in the delamination region and fail, if air at substrate temperature is applied directly on surface of TBC for cooling. It is expected that the safe cooling scenario would be a slow cool down of the entire system.

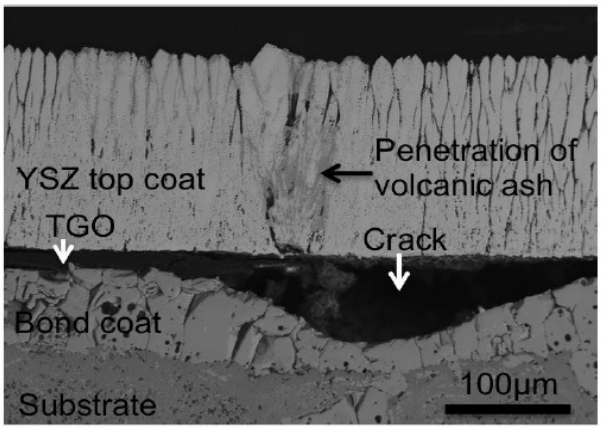

Figure 5-7: SEM image of the damaged YSZ top coat when infiltrated with volcanic ash at 1250℃ [15]

The experimental results obtained from [15] showed that delamination occurs in the TBC system upon being treated with volcanic ash at 1250℃ to a depth of 91 μm for a TBC with a thickness of 200 μm, Figure 5-7. The damage is severe and the YSZ (yttria-stabilized zirconia) top coat of the TBC is spalled due to volcanic ash infiltration. From the SEM image it is clear that the top coat could be entirely spalled and failed to protect the underlying substrate from further volcanic ash infiltration. Therefore, further effort is needed to develop crack models, in which the vertical cracks can kink out and then propagate parallel to the surface resulting in the delamination and eventually spallation off the TBC top coat, where the experimental results [15, 17] can be used to validate and improve such delamination models.

6. CONCLUSIONS

The delamination map of a TBC system degraded by volcanic ash infiltration was established based on fracture mechanics combining thermal gradient formulae. The degradation mechanism of volcanic ash on TBC was found to be similar to that for CMAS but could be more severe if the volcanic ash penetration rate to the top coat is faster, in addition to larger elastic moduli than that of the CMAS. The most severe cooling trajectory was used to identify the delamination map of the TBC system. A possible safest cooling trajectory was identified and recommended for operation of engines without causing TBC delamination. The allowable temperature windows inferred from the delamination map are needed to be compared with possible engine operation conditions for safe heating and cooling processes of TBC systems. The delamination map approach can be further explored to better design and develop more durable TBC systems.

ACKNOWLEDGEMENT

This work was supported by Air Defense Systems Program of National Research Council Canada.

REFERENCES

[1] T. M. Pollock and S. Tin, “Nickel-Based Superalloys for Advanced Turbine Engines: Chemistry, Microstructure and Properties,” *J. Propuls. Power*, vol. 22, no. 2, pp. 361–374, 2006.

[2] D. R. Clarke and C. G. Levi, “Materials Design for the Next Generation Thermal Barrier Coatings,”

Annu. Rev. Mater. Res., vol. 33, no. Figure 2, pp. 383–417, 2003.*[3] D. R. Clarke, M. Oechsner, and N. P. Padture, "Thermal-barrier coatings for more efficient gas-turbine engines," MRS Bull., vol. 37, no. October, pp. 891–898, 2012.*

[4] K. M. Grant, S. Krämer, J. P. a Löfvander, and C. G. Levi, "Cmas d," *Engineering*, no. March 2007.

[5] W. B. and P. Mechnich, "Braue and Mechnich - Recession of an EB-PVD YSZ Coated Turbine Blade by CaSO4 and Fe- Ti-rich CMAS-type Deposits.pdf." J. Am. Ceram. Soc 2011.

[6] C. Mercer, S. Faulhaber, a. G. Evans, and R. Darolia, "A delamination mechanism for thermal barrier coatings subject to calcium-magnesium-alumino-silicate (CMAS) infiltration," *Acta Mater.*, vol. 53, pp. 1029–1039, 2005.

[7] L. Li, N. Hitchman, and J. Knapp, "Failure of thermal barrier coatings subjected to CMAS attack," *J. Therm. Spray Technol.*, vol. 19, no. January, pp. 148–155, 2010.

[8] S. Krämer, S. Faulhaber, M. Chambers, D. R. Clarke, C. G. Levi, J. W. Hutchinson, and a. G. Evans, "Mechanisms of cracking and delamination within thick thermal barrier systems in aero-engines subject to calcium-magnesium-alumino-silicate (CMAS) penetration," *Mater. Sci. Eng. A*, vol. 490, pp. 26–35, 2008.

[9] G. Pujol, F. Ansart, J. P. Bonino, A. Malié, and S. Hamadi, "Step-by-step investigation of degradation mechanisms induced by CMAS attack on YSZ materials for TBC applications," *Surf. Coatings Technol.*, vol. 237, pp. 71–78, 2013.

[10] A. van L. W.Beele, G.Marijnissen, "The evolution of thermal barrier coatings-status and upcoming solutions for today's key issues." [Online]. Available: http://topaz.ethz.ch/function/web-het-secured/pdfs/Beele-99.pdf. [Accessed: 20-Apr-2015].

[11] a. G. Evans and J. W. Hutchinson, "The mechanics of coating delamination in thermal gradients," *Surf. Coatings Technol.*, vol. 201, pp. 7905–7916, 2007.

[12] E. Alejano, L.R. and Alonso, "Url @ Www.Google.Com," *International Journal of Rock Mechanics and Mining Science*, vol. 42. pp. 481–507, 2005.

[13] T. J. Grindle and F. W. Burcham, "Engine Damage to a NASA DC-8-72 Airplane From a High-Altitude Encounter With a Diffuse Volcanic Ash Cloud," no. August, 2003.

[14] X. Chen, "Calcium–magnesium–alumina–silicate (CMAS) delamination mechanisms in EB-PVD thermal barrier coatings," *Surface & Coatings Technology*, 2006. [Online]. Available: https://scholar.google.com/citations?user=sCQgjN0AAAAJ&hl=en. [Accessed: 17-Feb-2015].

[15] K. Lee, "Volcanic Ash Degradation on Thermal Barrier Coatings and Preliminary Fabrication of Protective Coatings," 2014.

[16] R. Siddique, "Volcanic Ash," *Aeronaut. Forecast. Handb.*, no. May, pp. 1–31, 2008.

[17] A. Aygun, N. Padture, S. Akbar, and G. Daehn, "Novel thermal barrier coatings (TBCs) that are resistant to high temperature attack by CMAS glassy deposits," vol. 2, 2008.

[18] M. Nakagawa, "Minerals in Volcanic Ash 1: Primary Minerals and Volcanic Glass," *Glob. Environ. Res.*, pp. 41–51, 2002.